

METHODOLOGY

Open Access



Application of a New Multiplexed Array for Rapid, Sensitive, Simultaneous and Quantitative Assessment of Spliced and Unspliced XBP1

Stuart Creedican^{1,2}, Aaron Talty², Stephen P. Fitzgerald³, Afshin Samali², Ciarán Richardson¹, Adrienne M. Gorman^{2†} and Kenneth Martin^{1*†}

Abstract

Background: IRE1 α -mediated unconventional splicing of XBP1 is emerging as a biomarker in several disease states and is indicative of activation of the unfolded protein response sensor IRE1. Splicing of *XBP1* mRNA results in the translation of two distinct XBP1 protein isoforms (XBP1s and XBP1u) which, due to post-translational regulation, do not correlate with mRNA levels. As both XBP1 isoforms are implicated in pathogenic or disease progression mechanisms there is a need for a reliable, clinically applicable method to detect them.

Methods: A multiplexed isoform-specific XBP1 array utilising Biochip array technology (BAT[™]) was assessed for specificity and suitability when using cell protein lysates. The array was applied to RIPA protein lysates from several relevant pre-clinical models with an aim to quantify XBP1 isoforms in comparison with RT-PCR or immunoblot reference methods.

Results: A novel reliable, specific and sensitive XBP1 biochip was successfully utilised in pre-clinical research. Application of this biochip to detect XBP1 splicing at the protein level in relevant breast cancer models, under basal conditions as well as pharmacological inhibition and paclitaxel induction, confirmed the findings of previous studies. The biochip was also applied to non-adherent cells and used to quantify changes in the XBP1 isoforms upon activation of the NLRP3 inflammasome.

Conclusions: The XBP1 biochip enables isoform specific quantification of protein level changes upon activation and inhibition of IRE1 α RNase activity, using a routine clinical methodology. As such it provides a research tool and potential clinical tool with a quantified, simultaneous, rapid output that is not available from any other published method.

Keywords: UPR, XBP1, Protein biochip, Quantitative XBP1 assessment

Introduction

The unfolded protein response (UPR) is a set of eukaryotic pathways activated by endoplasmic reticulum (ER) stress, which is defined by an accumulation of unfolded or misfolded proteins in the ER [1]. Canonically, detection of protein misfolding is dependent upon three ER-transmembrane receptors: inositol requiring enzyme 1 α (IRE1 α), protein

kinase RNA-activated (PKR)-like ER kinase (PERK) and activating transcription factor 6 (ATF6) [2]. The most studied and characterised of these ER stress sensors is IRE1. Activation of the ubiquitous IRE1 α isoform is dependent upon its autophosphorylation and subsequent oligomerisation which results in activation of its cytosolic RNase domain [3]. Signal transduction is possible through both kinase and RNase activity [4]. The most widely studied result of IRE1 α activation is the RNase-mediated unconventional splicing of *XBP1* pre-mRNA, resulting in the excision of 26 nucleotides and a frameshift in its open reading frame [5–7].

* Correspondence: kenneth.martin@randox.com

†Adrienne M. Gorman and Kenneth Martin contributed equally to this work.

¹Randox Teoranta, Meenmore, Dungloe, Co. Donegal, Ireland

Full list of author information is available at the end of the article



Translation of the conventionally spliced mRNA, *XBP1u*, results in a 29 kDa 232 amino acid protein, XBP1u, which has few known functions and is rapidly degraded in vitro [8, 9]. The most characterised action of XBP1u is as a negative regulator of XBP1s, though it has also been linked to regulation of the p53/p21 tumour suppression pathway [9, 10]. In contrast, translation of *XBP1s* mRNA (the result of unconventional IRE1 α mediated *XBP1* splicing) produces a potent transcription factor of 261 amino acids and ~ 55 kDa (Additional file 1: Figure S1A). XBP1s, along with other UPR regulated transcription factors, initiates a transcriptional programme aimed at reducing protein load through increased expression of the ER's protein folding or protein degradation machinery [11]. Increased splicing of *XBP1* has been associated with disease progression, therapy resistance and as a druggable target in a range of diseases [1].

The UPR is activated as a key pro-survival mechanism in many solid tumours in response to hypoxic and nutrient deprived conditions [1]. Constitutive activation of IRE1 α is proposed to confer a selective advantage onto cancer cells over neighbouring healthy and non-UPR activated cancer cells, with recent studies demonstrating up-regulated *XBP1* splicing in breast, pancreatic and ovarian cancer [12–14]. XBP1s upregulation in immune cells also contributes to immune evasion within the tumour micro-environment [15, 16]. Several conventional therapies routinely used in cancer treatment induce IRE1 α RNase activity, either providing pro-survival resistance or enhancing apoptotic effects [12, 17]. Small molecule mediated targeting of IRE1 α RNase activity is being investigated as an adjuvant therapy in several cancers [12, 18–20]. XBP1s has been implicated in the pathology in neurodegenerative disease models including Alzheimer's, Parkinson's and Huntington's diseases [21]. The consequences of IRE1 α activation are highly context dependent, with links to various molecular pathways including autophagy, apoptosis and prion resistance [22–24].

As therapies targeting the UPR enter clinical trials, and evidence for the use of XBP1s as a pathologically relevant biomarker grows, effective means of monitoring XBP1 splicing and expression of the XBP1 isoforms has become a clinical need. None of the methods currently employed for XBP1s or XBP1u detection are suitable for routine use in a clinical laboratory [25]. RT-PCR and RT-qPCR are often used to assess *XBP1* splicing, using primers flanking the spliced intron sequences where variant specificity is required [12]. Whilst more specialised laboratories can utilise RT-qPCR to obtain a quantitative measurement of XBP1s/XBP1u ratios, this method would have far less reliable results in a routine clinical setting. Factors such as extended sample preparation, potential for contamination and requirements for standardisation and

normalisation of results make RT-qPCR unsuitable for medium-high throughput in non-sterile clinical laboratories [25]. At the protein level, standard assessment of XBP1s (and less commonly XBP1u) is performed by immunoblotting. Medium to high throughput is not practical with this time-consuming and technically laborious method. Western blots are also largely unsuitable for quantification or inter-blot comparison with variation resulting from detection mechanisms, reagents and analysis methods [26–28].

Biochip Array Technology (BATTM) is commonly used in both clinical and research settings to simultaneously, quantitatively determine protein levels in serum and other biological matrices. The multiplexed sandwich immunoassay system provides a platform to assess multiple protein levels in a single sample [29, 30]. An assay system was proposed using the unique principles of sandwich-BAT to simultaneously capture the two XBP1 isoforms utilising their different C-termini, and detecting the captured protein using a Horse Radish Peroxidase (HRP) conjugated pan-detector targeted to their common N-terminus (Additional file 1: Figure S1B). Here we demonstrate the application of a biochip to simultaneous detection of the two XBP1 isoforms in models of breast cancer, non-adherent cells and inflammation.

Materials and Methods

Reagents

XBP1 Biochip assay kit was obtained from Randox Laboratories (XBP1 Array (EV4357), Randox Laboratories Ltd., Crumlin, UK). Thapsigargin (Tg) (Sigma-Aldrich, St. Louis, USA), Tunicamycin (Tm) (Sigma-Aldrich, St. Louis, USA), Brefeldin A (BFA) (Sigma-Aldrich, St. Louis, USA), Dithiothreitol (DTT) (Sigma-Aldrich, St. Louis, USA), 4 μ 8C (Sigma-Aldrich, St. Louis, USA), MKC-8866 (Prochem, St Pete Beach, USA), Paclitaxel (Taxol) (Sigma-Aldrich, St. Louis, USA), Lipopolysaccharide (LPS) (Sigma-Aldrich, St. Louis, USA) and Nigericin (Nig) (InvivoGen, San Diego, USA) were diluted in DMSO (Sigma-Aldrich, St. Louis, USA).

Biochip-Based Determination of XBP1s and XBP1u

XBP1s and XBP1u levels and raw signal were quantified using the Evidence Investigator analyser (EV3602, Randox Laboratories Ltd., UK). Signals from defined discrete test regions (DTRs) were detected using digital imaging technology as previously described [31]. The biochips were provided in wells within a carrier in a 3 \times 3 format (9 reaction wells per carrier). A carrier handling tray supplied with the system accommodated 6 carriers. The total assay protocol was performed according to manufacturer's instructions.

Briefly, RIPA lysed samples were diluted to 100 μ L in RIPA buffer followed by dilution to 200 μ L in XBP1

assay buffer and mixed well with gentle pipetting. Two hundred microliter of XBP1 assay diluent was then applied to the surface of the biochip followed by 200 μ L diluted sample or 100 μ L calibrator/control per well. Following a 60 min incubation at 37 °C, 370 RPM in a thermoshaker (Radox Laboratories Ltd., Crumlin, UK) liquid contents were removed with a sharp flick and washed in a 2X quick, 4X 2 min wash steps. Three hundred microliter of HRP-conjugated pan-XBP1 detector was applied to each well and another 60 min incubation at 37 °C, 370 RPM in a thermoshaker was performed. Following another wash as above 250 μ L of a 1:1 ratio of EV841 luminol and peroxide was applied to the surface of each biochip in a carrier and incubated away from direct light for 2 min. Carriers are then submitted to the Evidence Investigator, light emitted from each DTR is detected by the CCD camera and signal quantified by the instrument software.

Final values in pg/mg were obtained by dividing reported value (in pg) by total protein loaded per well, as determined by bicinchoninic acid (BCA) assay. Calibration curves, inferred values and goodness of fit were independently confirmed using R package *nplr* (0.1–7, Frederic Commo, <https://cran.r-project.org/web/packages/nplr/index.html>).

Cell Culture and Treatments

MCF10A (ATCC) cells were maintained in DMEM/F-12 (Sigma-Aldrich, St. Louis, USA) supplemented with 5% horse serum (Sigma-Aldrich, St. Louis, USA), 20 ng/mL epidermal growth factor (PeproTech, London, UK), 0.5 μ g/mL hydrocortisone (Sigma-Aldrich, St. Louis, USA), 100 ng/mL cholera toxin (Sigma-Aldrich, St. Louis, USA), 10 μ g/mL insulin (Sigma-Aldrich, St. Louis, USA), 50 U/mL penicillin, and 50 μ g/mL streptomycin (Sigma-Aldrich, St. Louis, USA). MCF7 cells (ECACC) were cultured in DMEM high glucose (Sigma-Aldrich, St. Louis, USA) supplemented with 10% foetal bovine serum (FBS), 0.01 mg/mL insulin (Sigma-Aldrich, St. Louis, USA), and 2 mM L-glutamine. MDA-MB-231 cells were cultured in DMEM high glucose (Sigma-Aldrich, St. Louis, USA) supplemented with 10% FBS, 50 U/mL penicillin, 50 μ g/mL streptomycin, and 2 mM L-glutamine. U937 and THP-1 (ATCC, Manassas, USA) cells were cultured in RPMI-1640 medium (Sigma-Aldrich, St. Louis, USA) supplemented with 10% FBS (Sigma-Aldrich, St. Louis, USA), 50 U/mL penicillin, 50 μ g/mL streptomycin (Sigma-Aldrich, St. Louis, USA), and 2 mM L-glutamine (Sigma-Aldrich, St. Louis, USA). All cells were cultured at 37 °C, 5% CO₂ in a humidified incubator and adherent cells seeded at an appropriate density 24 h prior to treatment. U937 cells were seeded at 5X10⁵ cells/mL and treated immediately while THP-1 cells were seeded at 1X10⁶ cells/mL and treated after 2 h.

Sample Preparation

Cells were washed once in ice cold phosphate-buffered saline (PBS) and then lysed in either RIPA buffer (Sigma-Aldrich, St. Louis, USA) with RocheSTOP® protease inhibitors (Roche, Basel, Switzerland) for protein analysis or directly lysed in TriReagent (Sigma-Aldrich, St. Louis, USA) as per manufacturer's instructions for RNA analysis.

Immunoblotting

Protein lysates were mixed with 5X Laemmli Buffer (0.3125 M Tris HCl (pH 6.8), 10% SDS, 50% glycerol, 25% 2-mercaptoethanol, 0.02% bromophenol blue) in a 1:4 ratio and boiled at 95 °C for 5 min. Samples were separated on an SDS polyacrylamide gel, transferred onto nitrocellulose membrane (GE Healthcare Life Sciences, Little Chalfont, UK) and blocked with 5% milk in Wash Buffer (Radox Laboratories Ltd., Crumlin, UK). Membranes were probed with commercial antibodies to spliced and unspliced XBP1 isoforms and actin (Sigma-Aldrich, St. Louis, USA, 1:5000). Anti-rabbit (Jackson ImmunoResearch, Cambridge, UK) and anti-mouse (Jackson ImmunoResearch, Cambridge, UK; Sigma-Aldrich, St. Louis, USA) HRP-conjugated secondary antibodies were incubated for 45–60 min and the signal was visualized using western blotting luminol reagent (Thermo-fisher, Waltham, USA; Perkin-Elmer, Waltham, USA).

RT-PCR

500–5000 ng of purified RNA was reverse transcribed using Superscript II (ThermoFisher, Waltham, USA). PCR was performed using GoTaq Green (MyBio Ltd., Kilkenny, Ireland) master mix and the following primers: FW XBP1 5'-GGA ACA GCA AGT GGT AGA-3', RV XBP1 5'-CTG GAG GGG TGA CAA CTG-3', FW GAPDH 5'-ACC ACA GTC CAT GCC ATC-3' and RV GAPDH 5'-TCC ACC ACC CTG TTG CTG-3'. Products were visualised on 3–4% Agarose in Tris Base, Acetic Acid, EDTA (TAE) buffer gels and stained with Midori green (ANACHEM, Leicester, UK).

Statistical Analysis

Statistical analysis was carried out using two-tailed t test with Welch's correction or one-way ANOVA where appropriate. $P < 0.05$ was considered statistically significant. Final analysis and calculations were performed in R version 3.5.1 "Feather Spray".

Results

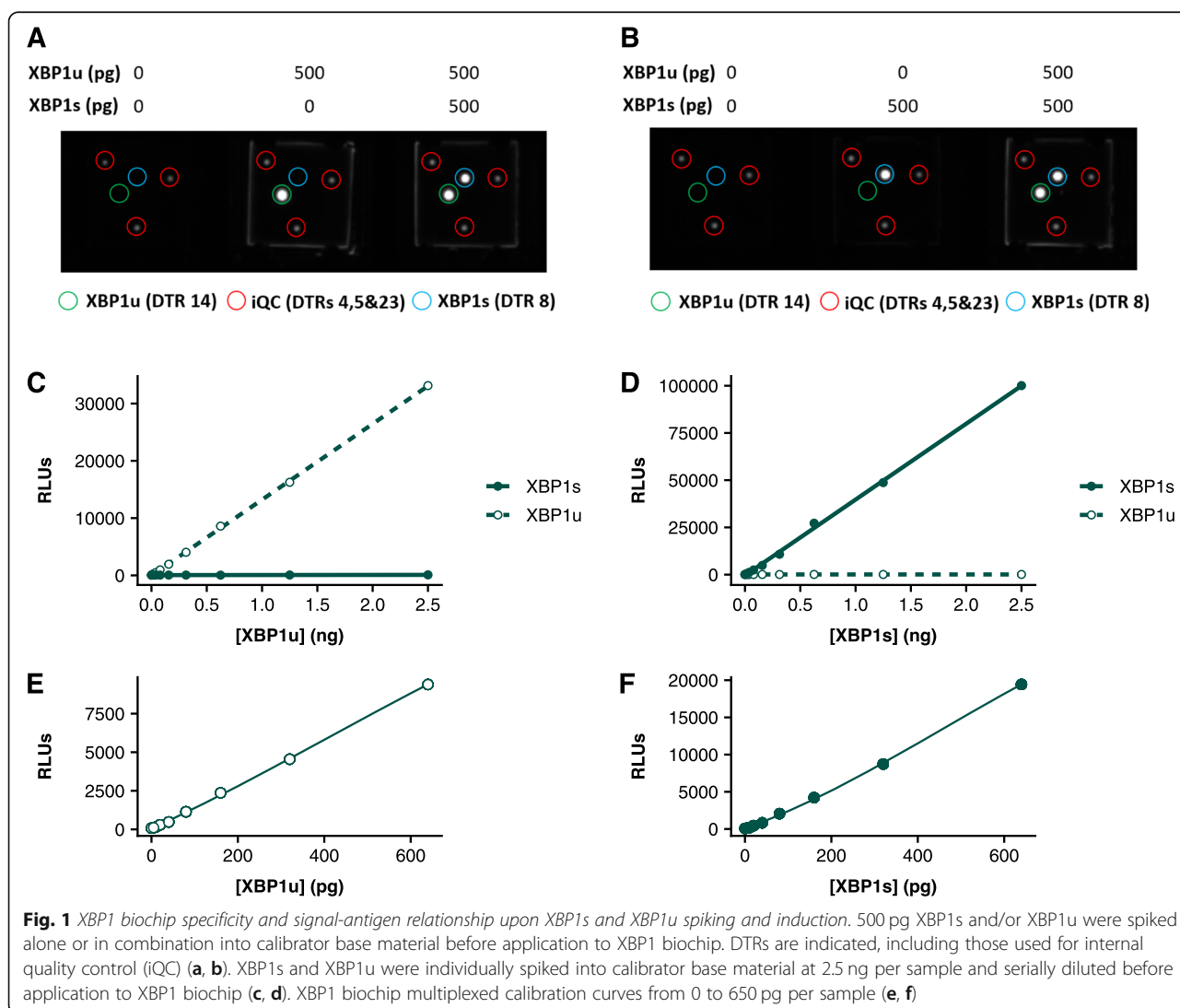
BAT multiplexed XBP1s and XBP1u assays are specific to their respective antigen and produce antigen dependent signal

To assess the XBP1 biochip's suitability and performance as a sandwich immunoassay in a multiplexed format the specificity and sensitivity of each assay was assessed.

Sandwich BAT assays utilise a solid state immobilised multiplexed ELISA based system as described previously [30]. BAT multiplexing of the two XBP1 isoforms requires the spotting of the two identified isoform specific capture antibodies into distinct DTRs on the ceramic biochip surface. Of the 25 DTRs present on a conventional biochip array three are used for internal quality control by the analysis software (DTRs 4, 5 and 23). DTRs 8 and 14 were chosen for XBP1u (Fig. 1a) and XBP1s analysis (Fig. 1b), respectively.

Clear signal with minimal background and cross-reactivity was observed upon spiking recombinant XBP1u (Fig. 1a) or XBP1s (Fig. 1b) into XBP1 assay calibrator base and assessing signal at the corresponding and other analyte's DTR. This DTR specificity and acceptable background signal (≤ 100 relative light units (RLU)) was observed even at 2.5 ng for both XBP1u

(Fig. 1c) and XBP1s (Fig. 1d, Additional file 2: Table S1). When spiked with 6.5 ng of XBP1u or XBP1s, cross reactivity at the other DTR was determined to be 0.61 and 0.30%, respectively. It was possible to obtain a reliable, antigen dependent signal with consistent and reproducible RLU observed at a 0–650 pg calibration range (Fig. 1e, f). The analytical sensitivity of each analyte was determined across 27 replicates and found to be 4.13 pg and 3.40 pg of XBP1u and XBP1u, respectively, while the functional sensitivity of each assay was 5.00 and 9.70 pg, respectively. Multiplexed intra-assay precision was determined at two levels (~ 15 –20 pg and ~ 55 –100 pg) for each analyte and was below 10% for XBP1s and 15% for XBP1u across 27 replicates. These results demonstrate that the XBP1 biochip can reliably quantify the XBP1 isoforms with high specificity.



XBP1 Biochip Detects XBP1 Splicing Upon Pharmacologically-Induced ER Stress

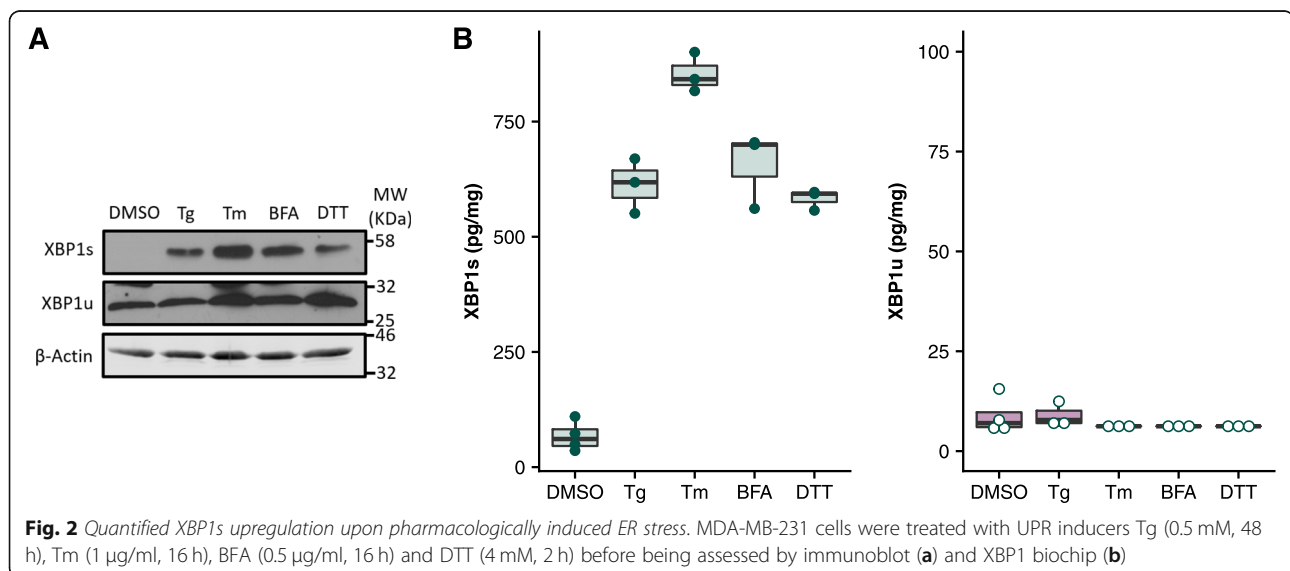
To confirm utility of the XBP1 biochip in cell lysates, a common model used to investigate ER stress mechanisms was utilised. Pharmacological induction of XBP1 splicing in *in vitro* and *in vivo* model systems is normally performed using a number of drugs with different mechanisms of action, all of which lead to an accumulation of misfolded proteins in the ER [32]. When MDA-MB-231 triple negative breast cancer (TNBC) cells were treated with Thapsigargin (Tg), Tunicamycin (Tm), Brefeldin A (BFA) or Dithiothreitol (DTT) an upregulation in XBP1s translation was observed (Fig. 2a). The XBP1 biochip was able to quantify the changes in XBP1 isoform expression, detecting the resultant XBP1 splicing at the protein level in RIPA lysates (Fig. 2b). A 10–30-fold increase in XBP1s/XBP1u ratio was detected by the XBP1 biochip when cells were treated with these commonly used treatments (Additional file 3: Figure S2) [12, 33, 34]. This confirms the XBP1 biochip is also suitable for detection and analysis of pharmacologically induced XBP1 splicing using treatments commonly utilised in investigating the effects of UPR activation.

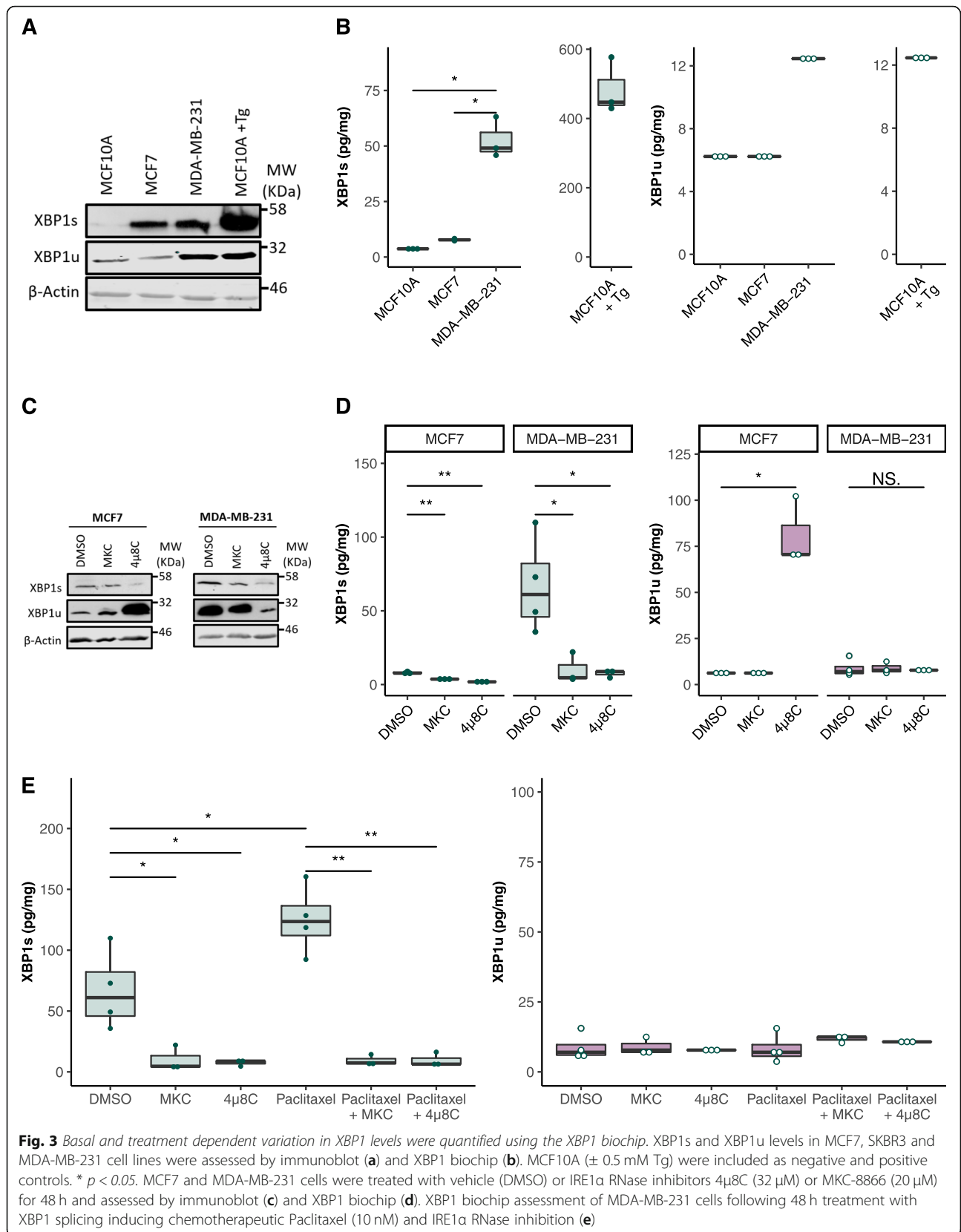
XBP1 Assessment Using BAT in Relevant Pre-Clinical Breast Cancer Cell Models

In order to test the XBP1 biochip in a physiologically relevant model, basal XBP1 levels were assessed in several breast cancer cell lines of different subtypes. Recent studies have shown constitutive activation of IRE1 α and resultant XBP1 splicing in basal-like (when stratified molecularly) and triple negative (when stratified by receptor expression) breast cancers. Other breast cancer subtypes can also display basal IRE1 α activity, but to a lesser extent [12].

Immunoblots confirmed previous results in XBP1 isoforms when comparing non-tumourigenic, Oestrogen receptor positive (ER+) and triple negative breast cancer cell lines (MCF10A, MCF7 and MDA-MB-231, respectively) (Fig. 3a). Using the XBP1 biochip we were able to observe and quantify these differences in XBP1 splicing at the protein level. TNBC cell line MDA-MB-231 displayed significantly higher basal XBP1 splicing than the non-tumourigenic or ER+ cell lines ($p = 0.014$ and 0.012 respectively). MCF7 cells also showed low level IRE1 α activity, with a mean XBP1s expression of 7.78 pg/mg (S.E. = 0.278 pg/mg). Reported XBP1u levels were consistently close to or at the functional sensitivity of the assay of 9.70 pg, indicating low basal expression levels (Fig. 3b).

To test if the XBP1 biochip has suitable sensitivity for research applications, IRE1 α RNase activity was pharmacologically inhibited. Inhibition of basal IRE1 α RNase activity has previously been shown to reduce tumour progression and size *in vitro* and *in vivo* in murine models [12]. Immunoblot was used to confirm a reduction in XBP1s both in MDA-MB-231 and MCF7 cells (which exhibit high and low basal levels of XBP1s, respectively) when using IRE1 α RNase inhibiting compounds 4 μ 8C and MKC-8866 (Fig. 3c). When quantified by the XBP1 biochip, 4 μ 8C appeared to be more potent than MKC-8866, but use of both compounds resulted in significant reduced XBP1s in MCF7 ($p = 0.004$ and $p = 0.008$) and MDA-MB-231 cells ($p = 0.035$ and $p = 0.033$). XBP1u protein levels remained largely unchanged in the MDA-MB-231 cells during IRE1 α inhibition ($p = 0.71$). However, MCF7 cells showed a significant upregulation of XBP1u protein upon 4 μ 8C treatment ($p = 0.019$) with expression levels averaging 81.1 pg/mg (Fig. 3d).





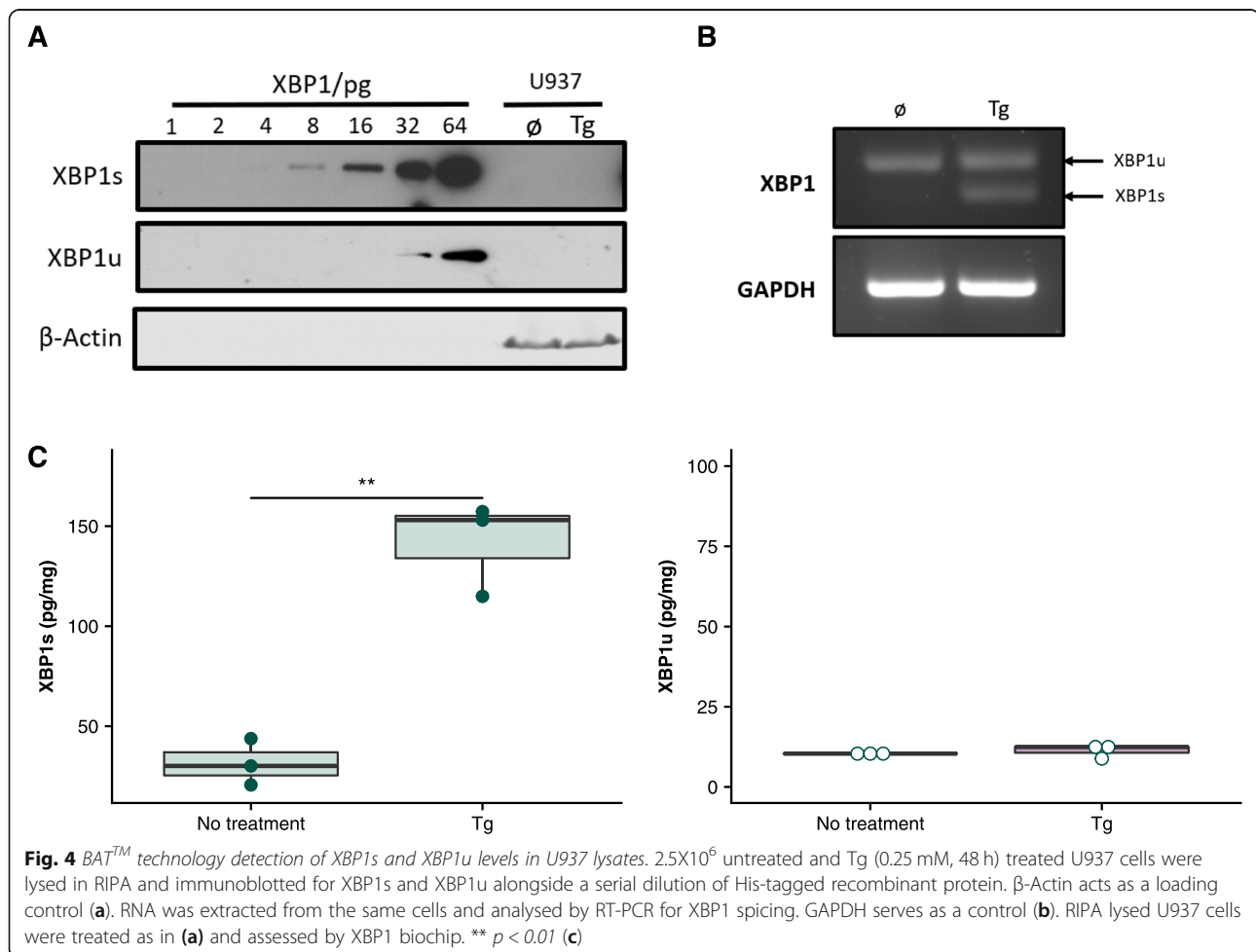
To assess the biochip's applicability in pre-clinical models a currently clinically approved modulator of IRE1 α activity was used. Paclitaxel, a commonly used chemotherapeutic in TNBC treatment, has also been shown to induce *XBP1* mRNA splicing [12]. Here we demonstrated that this increase in XBP1s was observed at the protein level, and that drug-induced changes in XBP1s were quantifiable with the XBP1 biochip. Paclitaxel treatment of MDA-MB-231 cells resulted in a modest but significant increase in XBP1s expression (66.9 ± 16.2 pg/mg to 125.0 ± 14.1 pg/mg, $p = 0.036$). This increase was completely ablated by pharmacological inhibition of IRE1 α RNase activity ($p < 0.01$ upon MKC-8866 or 4 μ 8C treatment). XBP1u levels showed no significant change with Paclitaxel combined with MKC-8866 or 4 μ 8C treatment (Fig. 3e).

These data indicate the utility of the XBP1 biochip in relevant pre-clinical models, showing its ability to detect basal and treatment induced levels of the XBP1 isoforms. Quantification of treatment-induced changes resulted in significant differences in XBP1s levels of cells treated

with IRE1 α inhibitors MKC-8866 and 4 μ 8C, and the clinically relevant ER stress inducer, Paclitaxel.

The XBP1 Biochip Shows Increased Ease of Use and Sensitivity in Non-adherent Model Systems

To determine if the XBP1 biochip had advantages over immunoblotting (the current standard method of protein level detection) a non-adherent cell model was assessed. Detecting the XBP1 isoforms by immunoblotting can be difficult, with many researchers preferring to detect *XBP1* splicing at the mRNA level [35]. Assessment of proteins of low abundance by immunoblotting can be particularly difficult in non-adherent cells [36]. This difficulty is typified by U937 cells, where, even after achieving exceptionally high sensitivity (low picogram levels), it was not possible to detect either XBP1 isoform in unstimulated or Tg stimulated samples by immunoblot, even with high protein input and prolonged exposure of the X-ray film (Fig. 4a). Detection difficulty was not due to lack of *XBP1* expression or IRE1 α RNase activity, as both presence and splicing of the transcript



were confirmed using RT-PCR (Fig. 4b). In contrast, the XBP1 biochip was able to detect significant changes in XBP1s protein expression in the same samples ($p = 0.0056$, Fig. 4c).

This demonstrates that the XBP1 biochip can be used to assess protein levels of both XBP1 isoforms even in model systems where XBP1 immunoblots can be difficult. The immunoblots shown here took approximately 72 h whilst total assessment using the XBP1 biochip took ~ 3 h.

NLRP3 Inflammasome Activation Associated XBP1 Splicing Is Detectable at the Protein Level with BATTM

To confirm the applicability of the XBP1 biochip in a relevant non-adherent model system pro-monocytic THP-1 cells were assessed upon inflammatory release. Talty et al. recently demonstrated that XBP1s splicing occurs upon activation the NLRP3 inflammasome and that inhibition of IRE1 α RNase activity could ablate NLRP3 mediated IL-1 β release [37].

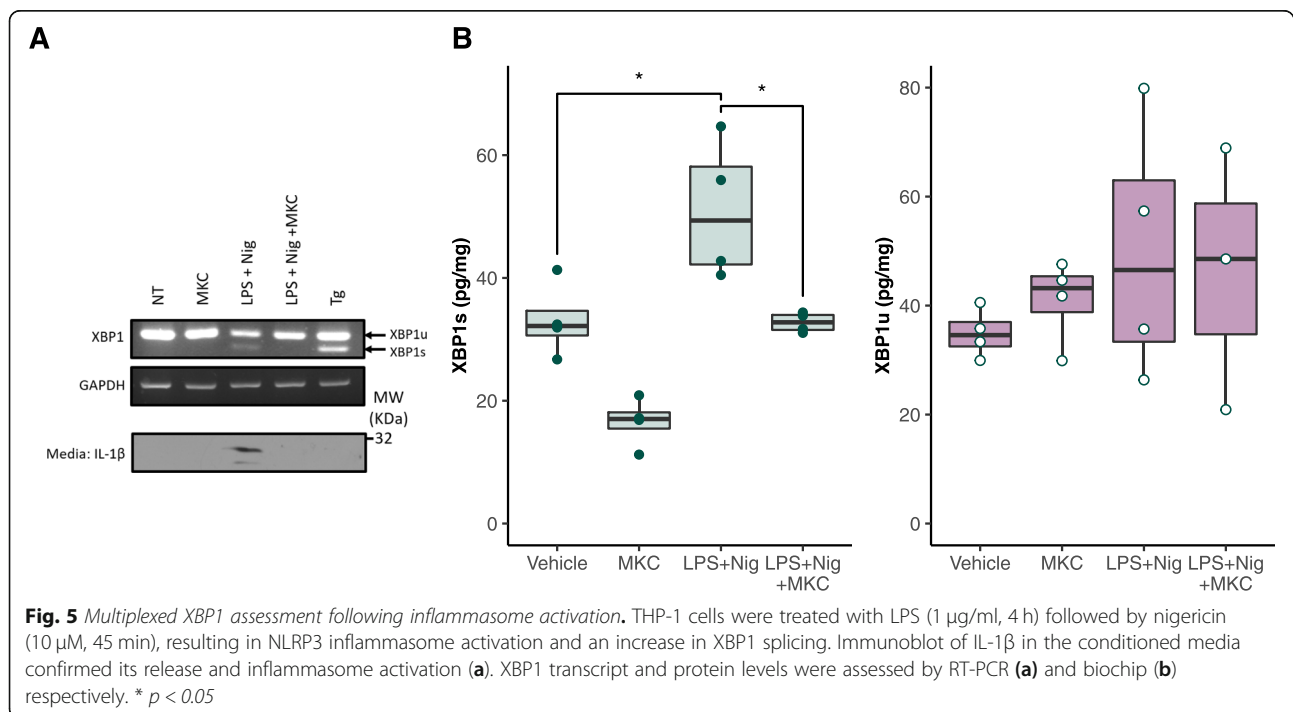
Here we demonstrate that this XBP1s splicing is detectable after only 4 h of LPS priming and 45 min of Nigericin secondary signal treatment and we replicate the previous observation that MKC-8866 mediated inhibition of IRE1 α RNase activity ablates IL-1 β release (Fig. 5a). The XBP1 biochip was used to detect and quantify these effects on XBP1 splicing at the protein level, detecting significant changes in XBP1s expression upon inflammasome activation ($p = 0.044$) and MKC-8866 mediated inhibition ($p = 0.048$). XBP1u levels

remained relatively high (mean = 46.2 pg/mg) but were largely unchanged by treatment (one-way ANOVA, $p = 0.408$) (Fig. 5b). Thus, the XBP1 biochip can detect XBP1 splicing following inflammatory stimulation and has identified a previously unreported high level of XBP1u protein in THP-1 cells.

Discussion

Here we have shown a rapid, reliable and quantitative method of detecting the XBP1 isoforms simultaneously at the protein level in several relevant model systems. This is the first time the individual XBP1 isoforms have been quantitatively assessed using a BATTM platform which is already available in pre-clinical and clinical settings in laboratories worldwide. As the IRE1 α mediated unconventional splicing of XBP1 pre-mRNA, resulting in the differential expression of the XBP1 isoforms, emerges as a biomarker and a druggable target in various disease states, this method will potentially allow researchers and clinicians alike to quickly determine basal expression, prognostic utility in multiple diseases and predict drug efficacy [12, 19, 38].

Isoform specific differential recognition has been shown to be a powerful tool in the multiplexing of the XBP1 assays, allowing for simultaneous detection of XBP1s and XBP1u in a single sample, with no apparent cross-reactivity of the other analyte, even when tested at levels far exceeding those observed in any of the samples used during development. This demonstrates that BATTM is highly suited to multiplexed analysis of



protein isoforms, even those of high similarity such as XBP1. The application of BATTM to detect protein isoforms has previously been demonstrated for simultaneous detection of ApoE isoforms in plasma, whilst the XBP1 biochip displays the utility of this technology in cell extracts [30]. Other enzyme-linked immunosorbent assay (ELISA) systems capable of XBP1 quantification are commercially available, but they fail to differentiate between the two isoforms and to our knowledge do not yet appear to have been used in any published works. In fact, use of these systems as an indirect measurement of XBP1s upregulation could lead to erroneous conclusions. This is demonstrated by MCF7 cells treatment with 4 μ 8C, where only an increase in total XBP1 would be observed and not a reduction in splicing and increased expression of XBP1u (Fig. 3d).

The XBP1 biochip has also demonstrated just how divergent protein levels of XBP1s and XBP1u are from their relative transcript levels. Whilst *XBP1s* transcript appears to correlate with protein levels of the isoform, XBP1u levels bear almost no resemblance to their transcript expression. In all but the most severe responses to ER stress *XBP1u* has remained the dominant transcript but at the protein level this pattern is reversed with much lower reported levels of XBP1u relative to XBP1s, particularly under ER stress [39]. Further exacerbating issues with this readout of IRE1 α -mediated effects is the use of *XBP1s*/*XBP1u* mRNA ratios, that are commonly used as a readout of IRE1 α activity in the literature [12]. At the protein level this ratio-based measurement of XBP1 isoform expression was suitable (though statistically less powerful) in the breast cancer models (Additional file 3: Figure S2 and Additional file 4: Figure S3) where XBP1u reported at low levels with little variation. A ratio measurement was also appropriate for Thapsigargin treated U937 cells (Additional file 5: Figure S4). However, this was not suitable for the THP1 model of inflammasome activation used (Additional file 6: Figure S5), where no significant changes in protein ratio were observed upon inflammasome activation despite the clear activation of IRE1 α RNase activity and resultant XBP1s expression. For many researchers this method of using mRNA ratios (or, in some cases, percentage of *XBP1s* of total *XBP1*) has not been considered an issue (e.g., those only looking for a functional readout of IRE1 α RNase activity). However, as the field develops and requires greater mechanistic explanations of downstream effects this will likely become an important issue for those requiring reliable, accurate measurement of the effector proteins of the IRE1-XBP1 pathway.

In spite of the low levels of both protein isoforms (relative to other conventional biomarkers and assays) it was still possible to quantify and detect significant changes in several relevant model systems. Quantification and simultaneous assessment also appeared to highlight the differential action of

MKC-8866 and 4 μ 8C in MCF7 cells. The greater inhibition observed upon application of 4 μ 8C when compared with MKC-8866 is proposed to be due to the higher concentration used (32 μ M vs 20 μ M respectively). Despite their structural similarity 4 μ 8C caused a large increase in XBP1u expression when compared with the untreated and MKC-8866 (and proposed to be much more specific) treated MCF7 cells. This is not the first time that 4 μ 8C has been proposed to have off-target effects with the potential to activate other pathways and demonstrates how multiplexed assessment can allow for mechanistic insights [40, 41]. In this case, simultaneous detection of XBP1u and XBP1s demonstrated that in MCF7 models 4 μ 8C not only reduces XBP1 splicing but also increases stability or expression of full length XBP1u.

Considering the reported antagonistic effects of XBP1u and XBP1s their simultaneous measurement could provide an increased understanding of their protein-protein relationship and how these interactions govern the downstream effects observed [9]. Previous studies focusing only on XBP1s expression may have failed to take XBP1u's known p53-p21, temporary translational arrest and inhibitory effects (beyond degradation) on XBP1s transcriptional activity into account [8–10, 42]. Here we have demonstrated how XBP1u protein varies greatly dependent on the model system used (and perhaps tissue assessed) while the implications of such protein level expression levels are yet to be explored.

Quantitative detection of basal and treatment-induced/inhibited XBP1 splicing, at the protein level in a high throughput amenable format presents an opportunity for pre-clinical and clinical applicability of XBP1 isoforms as an accessible biomarker. The XBP1 biochip also appears to show significant advantages over immunoblotting, not only in turn-around time, but in applicability to non-adherent model systems. Detection of protein level changes in circulating cells due to *XBP1* splicing and its inhibition could have great benefits in upcoming clinical trials, where non-invasive monitoring of IRE1 α or XBP1 targeting therapies efficacy will be required.

In comparison to other available methods, the XBP1 biochip allows for much greater in-depth analysis, providing simultaneous quantitative measurement of both isoforms. To date no other commercially available method can simultaneously quantify the two specific XBP1 protein isoforms while the XBP1 biochip is able to do this from an individual sample in approximately 3 h. This multiplexed quantitative analysis provides a tool for all researchers studying both or either of the XBP1 isoforms in a large variety of disease contexts, affording opportunities to monitor drug efficacy, confirm protein level changes in expression in relevant models and stratify patients for targeted therapies to name but a few applications.

Conclusion

In conclusion, we have shown here the development and utility of a rapid, sensitive, quantitative and multiplexed immunoassay array for detection of the two XBP1 isoforms. With a turn-around time of ~ 3 h, and simultaneous, quantitative analysis, it provides efficient and objective results which are not currently possible through any other commercially available method. We anticipate that this novel method of XBP1 isoform detection will make routine clinical screening feasible for multiple future diagnostic applications.

Supplementary information

Supplementary information accompanies this paper at <https://doi.org/10.1186/s12575-019-0111-3>.

Additional file 1: Figure S1. A sandwich immunoassay which captured the conventionally (*conv.*) spliced or frameshifted C-terminus of the XBP1 isoforms and a pan-detector of the common N-terminus was designed. Due to the unconventional splicing of XBP1 mRNA a translational frameshift occurs and results in XBP1 isoforms of differing length and C-terminal sequences (A). A biochip was proposed that utilised these different C-termini for simultaneous capture and the common N-terminus for detection (B).

Additional file 2: Table S1. Each DTR produces an antigen dependent signal not related to levels of the other analyte. 2.5 ng/ml of XBP1s and XBP1u were individually spiked into calibrator base and serially diluted. Acceptable background is ≤ 100 RLU in the non-target DTR.

Additional file 3: Figure S2. XBP1 protein ratio upon pharmacologically induced ER stress. XBP1 levels in MDA-MB-231 cells, expressed as a ratio of XBP1s (pg/mg)/XBP1u (pg/mg), upon induction with Tg (0.5 mM, 48 h), Tm (1 μ g/ml, 16 h), BFA (0.5 μ g/ml, 16 h) and DTT (4 mM, 2 h).

Additional file 4: Figure S3. Pre-clinical models of TNBC show results correlating with individual analyte assessment when assessed by XBP1 ratio. XBP1s and XBP1u levels expressed as a ratio of XBP1s (pg/mg)/XBP1u (pg/mg) in MCF7, SKBR3 and MDA-MB-231 cell lines (A). XBP1s and XBP1u levels expressed as a ratio of XBP1s (pg/mg)/XBP1u (pg/mg) in MCF7 and MDA-MB-231 cells treated with vehicle (DMSO) or IRE1 α RNase inhibitors 4 μ 8C (32 μ M) or MKC-8866 (20 μ M) for 48 h and assessed XBP1 biochip (B). XBP1s and XBP1u levels expressed as a ratio of XBP1s (pg/mg)/XBP1u (pg/mg) in MDA-MB-231 cells following 48 h treatment with XBP1 splicing inducing chemotherapeutic Paclitaxel (10 nM) and IRE1 α RNase inhibition (C).

Additional file 5: Figure S4. Loading of lysate and diluted recombinant protein in Fig. 4 was confirmed by silver staining. Recombinant XBP1 isoforms were diluted in ddH₂O before addition of 5X Laemmli buffer. A serial dilution was run alongside unstimulated and 0.5 μ M Tg stimulated U937 lysate and silver stained (A). RIPA lysed U937 cells were treated as in (A) and assessed by XBP1 biochip. XBP1s and XBP1u levels expressed as a ratio of XBP1s (pg/mg)/XBP1u (pg/mg). ** $p < 0.01$ (B).

Additional file 6: Figure S5. Assessment of XBP1s/u protein ratio is not indicative of IRE1 α activity in THP-1 cells. XBP1s and XBP1u levels in THP-1 cells (stimulated to induce NLRP3 inflammasome activation and inhibited by MKC-8866) expressed as a ratio of XBP1s (pg/mg)/XBP1u (pg/mg). ** $p < 0.01$.

Abbreviations

ATF6: Activating Transcription Factor 6; BAT: Biochip Array Technology; BCA: Bicinchoninic acid; DTR: Discrete Test Region; ELISA: Enzyme-linked immunosorbent assay; ER: Endoplasmic Reticulum; HRP: Horse Radish Peroxidase; IRE1: Inositol Requiring Enzyme 1; NLRP3: NACHT, LRR and PYD domains; PERK: Protein kinase RNA-activated (PKR)-like ER Kinase; RLU: Relative Light Unit; TAE: Tris Base, Acetic Acid, EDTA; TNBC: Triple

Negative Breast Cancer; UPR: Unfolded Protein Response; XBP1: X-Box binding protein 1

Acknowledgements

The authors would like to thank Dr. MariLuz Rodrigues for helpful discussion.

Authors' contributions

SC planned performed and analysed all experiments unless otherwise stated. AT and SC performed experiments described in Fig. 5. KM, CR, SPF, AG and AS provided project supervision and critical review of the manuscript. SC wrote the manuscript. All authors read and approved the final manuscript.

Funding

This project received funding from the European Union's Horizon 2020 research and innovation programme under the Marie Skłodowska-Curie grant agreement No. 675448 (TRAIN-ERS).

Availability of data and materials

The datasets measured and analyzed during the study are available from the corresponding authors upon reasonable request.

Ethics approval and consent to participate

This article does not contain any studies with human participants.

Consent for publication

All the authors have accepted responsibility for the entire content of this submitted manuscript and approved submission.

Competing interests

AG and AS are cofounders of Cell Stress Discoveries, Ltd., there no conflicting interests. CR, KM are employed by Randox Teoranta, SPF is employed by Randox Holdings. The funding organization played no role in the study design; in the collection, analysis, and interpretation of data; in the writing of the report; or in the decision to submit the report for publication.

Author details

¹Randox Teoranta, Meenmore, Dungloe, Co. Donegal, Ireland. ²Apoptosis Research Centre, National University of Ireland Galway, University Road, Galway H91 TK33, Ireland. ³Randox Laboratories Ltd., 55 Diamond Road, Crumlin, Co. Antrim, Northern Ireland BT29 4QY.

Received: 6 September 2019 Accepted: 31 October 2019

Published online: 15 November 2019

References

- Almanza A, Carlesso A, Chintia C, Creedican S, Doultinos D, Leuzzi B, et al. Endoplasmic reticulum stress signalling – from basic mechanisms to clinical applications. *FEBS J.* 2019;286(2):241–78. <https://doi.org/10.1111/febs.14608>.
- Schardt JA, Eyholzer M, Timchenko NA, Mueller BU, Pabst T. Unfolded protein response suppresses CEBPA by induction of calreticulin in acute myeloid leukaemia. *J Cell Mol Med.* 2010;14(6 B):1509–19.
- Bouchecareilh M, Higa A, Fribourg S, Moenner M, Chevet E. Peptides derived from the bifunctional kinase/RNase enzyme IRE1 α modulate IRE1 α activity and protect cells from endoplasmic reticulum stress. *FASEB J.* 2011; 25(9):3115–29. <https://doi.org/10.1096/fj.11-182931>.
- Urano F, Bertolotti A, Ron D. IRE1 and efferent signaling from the endoplasmic reticulum. *J Cell Sci.* 2000;113(21):3697 LP–3702 Available from: <http://jcs.biologists.org/content/113/21/3697.abstract>.
- Nandy A, Saenz-Méndez P, Gorman AM, Samali A, Eriksson LA. Homology model of the human tRNA splicing ligase RtcB. *Proteins Struct Funct Bioinform.* 2017;85(11):1983–93. <https://doi.org/10.1002/prot.25352>.
- Sha H, He Y, Chen H, Wang C, Zenno A, Shi H, et al. The IRE1 α -XBP1 pathway of the unfolded protein response is required for adipogenesis. *Cell Metab.* 2009;9(6):556–64 Available from: <https://www.ncbi.nlm.nih.gov/pubmed/19490910>.
- Calton M, Zeng H, Urano F, Till JH, Hubbard SR, Harding HP, et al. IRE1 couples endoplasmic reticulum load to secretory capacity by processing the XBP-1 mRNA. *Nature.* 2002;415:92. <https://doi.org/10.1038/415092a>.
- Chen C, Malchus NS, Hehn B, Stelzer W, Avci D, Langosch D, et al. Signal peptide peptidase functions in ERAD to cleave the unfolded protein response regulator XBP 1 u. *EMBO J.* 2014;33(21):2492–506.

9. Guo F, Lin EA, Liu P, Lin J, Liu C. XBP1U inhibits the XBP1S-mediated upregulation of the iNOS gene expression in mammalian ER stress response. *Cell Signal*. 2010;22(12):1818–28. <https://doi.org/10.1016/j.cellsig.2010.07.006>.
10. Huang C, Wu S, Ji H, Yan X, Xie Y, Murai S, et al. Identification of XBP1-u as a novel regulator of the MDM2 / p53 axis using an shRNA library; 2017. p. 1–15.
11. Ron D, Walter P. Signal integration in the endoplasmic reticulum unfolded protein response. *Nat Rev Mol Cell Biol*. 2007;8:519. <https://doi.org/10.1038/nrm2199>.
12. Logue SE, McGrath EP, Cleary P, Greene S, Mnich K, Almanza A, et al. Inhibition of IRE1 RNase activity modulates the tumor cell secretome and enhances response to chemotherapy. *Nat Commun*. 2018;9(1). <https://doi.org/10.1038/s41467-018-05763-8>.
13. Thakur PC, Miller-Ocun JL, Nguyen K, Matsuda R, Singhi AD, Zeh HJ, et al. Inhibition of endoplasmic-reticulum-stress-mediated autophagy enhances the effectiveness of chemotherapeutics on pancreatic cancer. *J Transl Med*. 2018; 16(1):190 Available from: <https://www.ncbi.nlm.nih.gov/pubmed/29986726>.
14. Zhang L, Hapon MB, Goyeneche AA, Srinivasan R, Gamarra-Luques CD, Callegari EA, et al. Mifepristone increases mRNA translation rate, triggers the unfolded protein response, increases autophagic flux, and kills ovarian cancer cells in combination with proteasome or lysosome inhibitors. *Mol Oncol*. 2016;10(7):1099–117 Available from: <https://www.ncbi.nlm.nih.gov/pubmed/27233943>. 2016/05/17.
15. Rodvold JJ, Chiu KT, Hiramatsu N, Nussbacher JK, Galimberti V, Mahadevan NR, Willert K, Lin JH, Zanetti M. Intercellular transmission of the unfolded protein response promotes survival and drug resistance in cancer cells. *Sci Signal*. 2017;10(482):eaah7177.
16. Cubillos-Ruiz JR, Bettigole SE, Glimcher LH. Molecular Pathways: Immunosuppressive Roles of IRE1 α -XBP1 Signaling in Dendritic Cells of the Tumor Microenvironment. *Clin Cancer Res*. 2016;22(9):2121–6 Available from: <https://www.ncbi.nlm.nih.gov/pubmed/26979393>. 2016/03/15.
17. Csizmar CM, Kim DH, Sachs Z. The role of the proteasome in AML. *Blood Cancer J*. 2016;6(12):e503. <https://doi.org/10.1038/bcj.2016.112>.
18. Wilhelm T, Bick F, Peters K, Mohta V, Tirosh B, Patterson JB, et al. Inflection of proteotoxic stresses by impairment of the unfolded protein response or proteasomal inhibition as a therapeutic strategy for mast cell leukemia. *Oncotarget*. 2018;9(3):2984–3000 Available from: <http://www.oncotarget.com/fulltext/23354>.
19. Sun H, Lin D-C, Guo X, Masouleh BK, Gery S, Cao Q, et al. Inhibition of IRE1 α -driven pro-survival pathways is a promising therapeutic application in acute myeloid leukemia. *Oncotarget*. 2014;7(3(8 Supplement)):2030 Available from: <http://www.ncbi.nlm.nih.gov/pubmed/26934650%5Cn>, <http://www.oncotarget.com/abstract/7702>.
20. Wilhelm T, Bick F, Peters K, Mohta V, Tirosh B, Patterson JB, et al. Inflection of proteotoxic stresses by impairment of the unfolded protein response or proteasomal inhibition as a therapeutic strategy for mast cell leukemia. *Oncotarget*. 2017;9(3):2984–3000 Available from: <https://www.ncbi.nlm.nih.gov/pubmed/29423023>.
21. Schepers W, Hoozemans JJM. The unfolded protein response in neurodegenerative diseases: a neuropathological perspective. *Acta Neuropathol*. 2015;130(3):315–31 Available from: <https://www.ncbi.nlm.nih.gov/pubmed/26210990>. 2015/07/26.
22. Hughes D, Mallucci GR. The unfolded protein response in neurodegenerative disorders – therapeutic modulation of the PERK pathway. *FEBS J*. 2019;286(2):342–55. <https://doi.org/10.1111/febs.14422>.
23. Gomez-Velazquez M, Rincon-Limas DE, Casas-Tinto S, Zhang Y, Fernandez-Funez P, Sanchez-Garcia J. The ER stress factor XBP1s prevents amyloid- β neurotoxicity. *Hum Mol Genet*. 2011;20(11):2144–60. <https://doi.org/10.1093/hmg/ddr100>.
24. Desdin-Micó G, Mittelbrunn M. Role of exosomes in the protection of cellular homeostasis. *Cell Adhes Migr*. 2017;11(2):127–34. <https://doi.org/10.1080/19336918.2016.1251000>.
25. Sanders R, Mason DJ, Foy CA, Huggett JF. Considerations for accurate gene expression measurement by reverse transcription quantitative PCR when analysing clinical samples. *Anal Bioanal Chem*. 2014;406(26):6471–83. Available from: <https://www.ncbi.nlm.nih.gov/pubmed/24858468>. 2014/05/25.
26. Luo H, Rankin GO, Straley S, Chen YC. Sensitivity in Western blotting. *J Pharmacol Toxicol Methods*. 2012;64(3):233–7.
27. Mathews ST, Plaisance EP, Kim T. Imaging Systems for Westerns: Chemiluminescence vs. infrared detection BT - protein blotting and detection: methods and protocols. In: Kurien BT, Scofield RH, editors. . Totowa: Humana Press; 2009. p. 499–513. https://doi.org/10.1007/978-1-59745-542-8_51.
28. Degasperis A, Birtwistle MR, Volinsky N, Rauch J, Kolch W, Kholodenko BN. Evaluating Strategies to Normalise Biological Replicates of Western Blot Data. *PLoS One*. 2014;9(1):e87293. <https://doi.org/10.1371/journal.pone.0087293>.
29. Veitinger M, Oehler R, Umlauf E, Baumgartner R, Schmidt G, Gerner C, et al. A platelet protein biochip rapidly detects an Alzheimer's disease-specific phenotype. *Acta Neuropathol*. 2014;128(5):665–77 Available from: <https://www.ncbi.nlm.nih.gov/pubmed/25248508>. 2014/09/24.
30. Badrnya S, Doherty T, Richardson C, McConnell RI, Lamont JV, Veitinger M, FitzGerald SP, Zellner M, Umlauf E. Development of a new biochip array for APOE4 classification from plasma samples using immunoassay-based methods. *Clin Chem Lab Med*. 2018;56(5):796–802.
31. McAleer D, McPhillips FM, FitzGerald SP, McConnell RI, Rodriguez M. Application of Evidence InvestigatorTM for the Simultaneous Measurement of Soluble Adhesion Molecules: L-, P-, E- Selectins, VCAM-1, ICAM-1 in a Biochip Platform. *J Immunoassay Immunochem*. 2006;27(4):363–78. <https://doi.org/10.1080/15321810600862298>.
32. Osowski CM, Urano F. Measuring ER stress and the unfolded protein response using mammalian tissue culture system. *Methods Enzymol*. 2011; 490:71–92 Available from: <https://www.ncbi.nlm.nih.gov/pubmed/21266244>.
33. de Galarreta MR, Navarro A, Ansorena E, Garzón AG, Mòdol L, López-Zabalza MJ, et al. Unfolded protein response induced by Brefeldin A increases collagen type I levels in hepatic stellate cells through an IRE1 α , p38 MAPK and Smad-dependent pathway. *Biochim Biophys Acta, Mol Cell Res*. 2016; 1863(8):2115–23 Available from: <http://www.sciencedirect.com/science/article/pii/S0167488916301306>.
34. Calfon M, Zeng H, Urano F, Till JH, Stevan RH, Harding HP, et al. IRE1 couples endoplasmic reticulum load to secretory capacity by processing the XBP-1 mRNA. *Nature*. 2002;415(January):92–6 Available from: <http://www.wormbase.org/db/misc/paper?name=WBpaper00005036>.
35. Kennedy D, Samali A, Jäger R. Methods for studying ER stress and UPR markers in human cells. *Methods Mol Biol*. 2015;1292:3–18.
36. Martinon F, Chen X, Lee A-H, Glimcher LH. TLR activation of the transcription factor XBP1 regulates innate immune responses in macrophages. *Nat Immunol*. 2010;11(5):411–8 Available from: <https://www.ncbi.nlm.nih.gov/pubmed/20351694>. 2010/03/28.
37. Talty A, Deegan S, Lujic M, Mnich K, Naicker SD, Quandt D, et al. Inhibition of IRE1 α RNase activity reduces NLRP3 inflammasome assembly and processing of pro-IL1 β . *Cell Death Dis*. 2019;10(9):622. <https://doi.org/10.1038/s41419-019-1847-z>.
38. Shi W, Chen Z, Li L, Liu H, Zhang R, Cheng Q, et al. Unravel the molecular mechanism of XBP1 in regulating the biology of cancer cells. *J Cancer*. 2019;10(9):2035–46 Available from: <https://www.ncbi.nlm.nih.gov/pubmed/31205564>.
39. van Schadewijk A, van't Wout EFA, Stolk J, Hiemstra PS. A quantitative method for detection of spliced X-box binding protein-1 (XBP1) mRNA as a measure of endoplasmic reticulum (ER) stress. *Cell Stress Chaperones*. 2012; 17(2):275–9 Available from: <https://www.ncbi.nlm.nih.gov/pubmed/22038282>. 2011/10/31.
40. Stewart C, Estrada A, Kim P, Wang D, Wei Y, Gentile C, et al. Regulation of IRE1 α by the small molecule inhibitor 4 μ 8c in hepatoma cells. *Endoplasmic Reticulum Stress Dis*. 2017;4(1):1–10 Available from: <https://www.ncbi.nlm.nih.gov/pubmed/29098149>. 2017/04/27.
41. Chan SMH, Lowe MP, Bernard A, Miller AA, Herbert TP. The inositol-requiring enzyme 1 (IRE1 α) RNase inhibitor, 4 μ 8c, is also a potent cellular antioxidant. *Biochem J*. 2018;475(5):923 LP–929 Available from: <http://www.biochemj.org/content/475/5/923.abstract>.
42. Shanmuganathan V, Schiller N, Magoulopoulou A, Cheng J, Braunger K, Cymer F, et al. Structural and mutational analysis of the ribosome-arresting human XBP1u. *Elife*. 2019;8:e46267. <https://doi.org/10.7554/eLife.46267> Hegde RS, Ron D, Mankin A, editors.

Publisher's Note

Springer Nature remains neutral with regard to jurisdictional claims in published maps and institutional affiliations.